

REPORT DOCUMENTATION PAGE
*Form Approved
OMB No. 0704-0188*

The public reporting burden for this collection of information is estimated to average 1 hour per response, including the time for reviewing instructions, searching existing data sources, gathering and maintaining the data needed, and completing and reviewing the collection of information. Send comments regarding this burden estimate or any other aspect of this collection of information, including suggestions for reducing the burden, to the Department of Defense, Executive Services and Communications Directorate (0704-0188). Respondents should be aware that notwithstanding any other provision of law, no person shall be subject to any penalty for failing to comply with a collection of information if it does not display a currently valid OMB control number.

PLEASE DO NOT RETURN YOUR FORM TO THE ABOVE ORGANIZATION.

1. REPORT DATE (DD-MM-YYYY)	2. REPORT TYPE	3. DATES COVERED (From - To)		
4. TITLE AND SUBTITLE		5a. CONTRACT NUMBER		
		5b. GRANT NUMBER		
		5c. PROGRAM ELEMENT NUMBER		
6. AUTHOR(S)		5d. PROJECT NUMBER		
		5e. TASK NUMBER		
		5f. WORK UNIT NUMBER		
7. PERFORMING ORGANIZATION NAME(S) AND ADDRESS(ES)			8. PERFORMING ORGANIZATION REPORT NUMBER	
9. SPONSORING/MONITORING AGENCY NAME(S) AND ADDRESS(ES)			10. SPONSOR/MONITOR'S ACRONYM(S)	
			11. SPONSOR/MONITOR'S REPORT NUMBER(S)	
12. DISTRIBUTION/AVAILABILITY STATEMENT				
13. SUPPLEMENTARY NOTES				
14. ABSTRACT				
15. SUBJECT TERMS				
16. SECURITY CLASSIFICATION OF:		17. LIMITATION OF ABSTRACT	18. NUMBER OF PAGES	19a. NAME OF RESPONSIBLE PERSON
a. REPORT	b. ABSTRACT	c. THIS PAGE		19b. TELEPHONE NUMBER (Include area code)



College of Optics and Photonics
CREOL & FPCE

Contract: **FA 95500510397**

Title: **Femtosecond Laser Passivation of GaAs detector material**

Report: **2007 Final Report**

Agency: **AFOSR**
Directorate of Physics and Electronics, AFOSR/NE
4015 Wilson Blvd, Room 713, Arlington VA 22203-1954
Tel 703 696 8569, DSN 426 8569

Program Manager: **Dr Anne Matsumura**
Tel 703 696 6204

Originating Agent: **Dr Dennis Healy**
Originating Agency: **DARPA, Microsystems Technology Office**
Agency Address: 3701, North Fairfax Dr., Arlington, VA, 22203
Tel: 571 218 4330, Fax: 703 696 2206, email: dennis.healy@darpa.mil

Performers: **Martin Richardson, Glenn Boreman, Univ. of Centr. Florida, Orlando, FL**
Kathleen Richardson, Clemson University, SC,

P.I.: **Martin Richardson**
Townes Laser Institute, CREOL – College of Optics
University of Central Florida
4000 Central Florida Blvd., Orlando, Fl, 32816-2700
Tel: 407 823 6819, Fax: 407 823 3570, email: mcr@creol.ucf.edu

1. Introduction

Passivation is intent to change the material in an way that dangling bonds become repaired and the noise due to the half-bound electrons decreases. To understand the physical and structural changes during and after passivation a general understanding of the electrical behavior of the photoconductors is required.

In this program,

- ◊ We will investigate for the bond modification in GaAs with fs lasers and its modification to signal response and electrical noise of the semiconductor devices
- ◊ We will systematically evaluate changes in noise behavior (PSD) in well characterized GaAs detector material to assess the influence of various laser process parameters (λ , dose, etc.), prior to, and immediately following exposure.
- ◊ We will relate noise variation (as a function of frequency range) to corresponding structural and electronic changes.

2. Experimental Facilities

2.1 Single Frequency Light Source

To generate this sinusoidal signal, a laser-diode setup consisting of a laser-diode with $\lambda=785$ nm, a Lightwave diode mount (LDM-4407), a laser-diode controller (model LDC-3700 series) and a waveform generator to generate the sinusoidal function was constructed. A schematic of the setup is shown in Figure 1. The shape and modulation frequency of the emitted waveform were controlled by the output of the waveform generator, which had a frequency range of 1.5 to 10kHz. This signal was then used by the LD controller to modulate the intensity of the laser diode. The average power was set to $P_{LD} \approx 50$ mW.

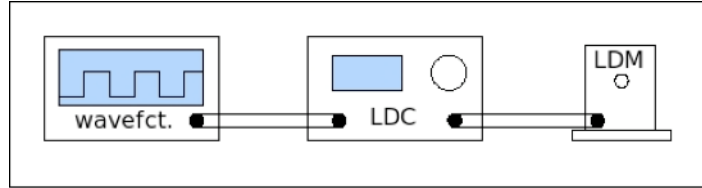


Figure 1 - Diode-Setup, Wavefct. : Waveform-generator; LDC: Laser-Diode-Controller; LDM: Laser-Diode-Mount with diode

2.2 Photoconductor bias source

An electric amplifier circuit was designed to intensify both signal and noise coming from the photoconductor above the noise level of the used oscilloscope. The amplifier also reduces fluctuations of the bias-voltage of the measurement circuit by using batteries as source instead of wall-plug power-sources and shields the signal against surrounding radiation.

2.3 2 μ m Fiber Laser Source

An advanced signal analysis workstation containing a long wavelength light source was constructed to test the mid-IR response of the fabricated photoconductors. A new fiber laser source with a wavelength of $\lambda=2\mu$ m was developed in-house for this purpose. The emission from the fiber laser contained both 2 μ m radiation as well as 790nm radiation from the pump source. The separation of pump light and the IR-fiber laser light was realized by three dichroic mirrors which were highly reflective $\lambda=2\mu$ m and highly transmissive ($R_{pump} < 1\%$) for the pump light. The product of the reflectivity of these mirrors defines a total reflectivity for the pump light of $R_{total-pump} < 10^{-6}$. Thus, only 2 μ m light was incident on the photoconductors. The power of the laser output was set to $P_{2\mu m} \approx 35$ mW. Direct modulation of the laser output by the pump intensity was attempted, but did not lead to a stable laser cavity. Therefore, a chopper wheel was used to modulate the light as in previous experiments, despite the undesirable

presence of harmonics in the signal. The frequency of the chopper wheel was variable over the region of $f_{L-2\mu m}=1$ kHz to $f_{H-2\mu m}=2.5$ kHz and was set to $f_{2\mu m}=1.5$ kHz. The electric response of photoconductor device was analyzed by same setup which was used for the irradiation in the visible range with the laser-diode. A schematic is shown in Figure 2. The time domain signal and Fourier-transformed frequency response were analyzed using the set up shown in Figure 3.

2.4 Cryogenically Cooled Chamber

A setup to realize ultra-low-temperature (down to $T=15^{\circ}\text{K}$) dark current and noise measurements in a low thermal energy environment was designed. A vacuum-cryo-chamber from CRYO-Tech was used, which provided dynamic thermal control from $T=15^{\circ}\text{K}$ up to room temperature at $T=300^{\circ}\text{K}$. A highly shielded signal cable was used to further reduce noise in the system from external radiation. A custom-made mount was constructed to allow the cable to pass through the wall of vacuum chamber to an external oscilloscope.

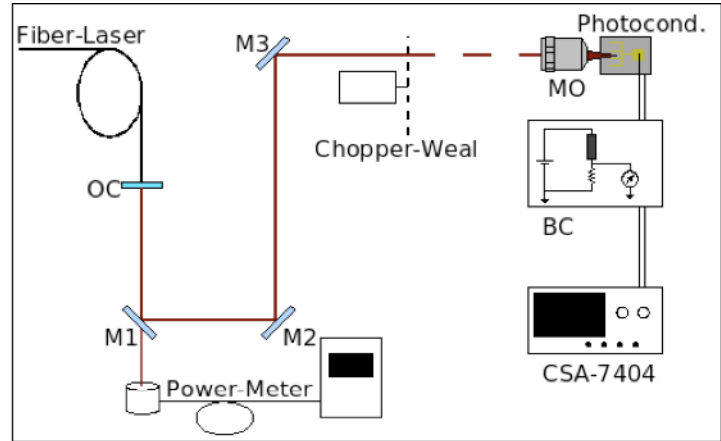


Figure 2 - Mid-IR-Setup, OC: Output-Coupler Fiber-Laser; M1-M3: HR mirrors for 2mm; MO: Microscope Objective; BC: Bias-Circuit Fig.2; CSA-7404: Oscilloscope

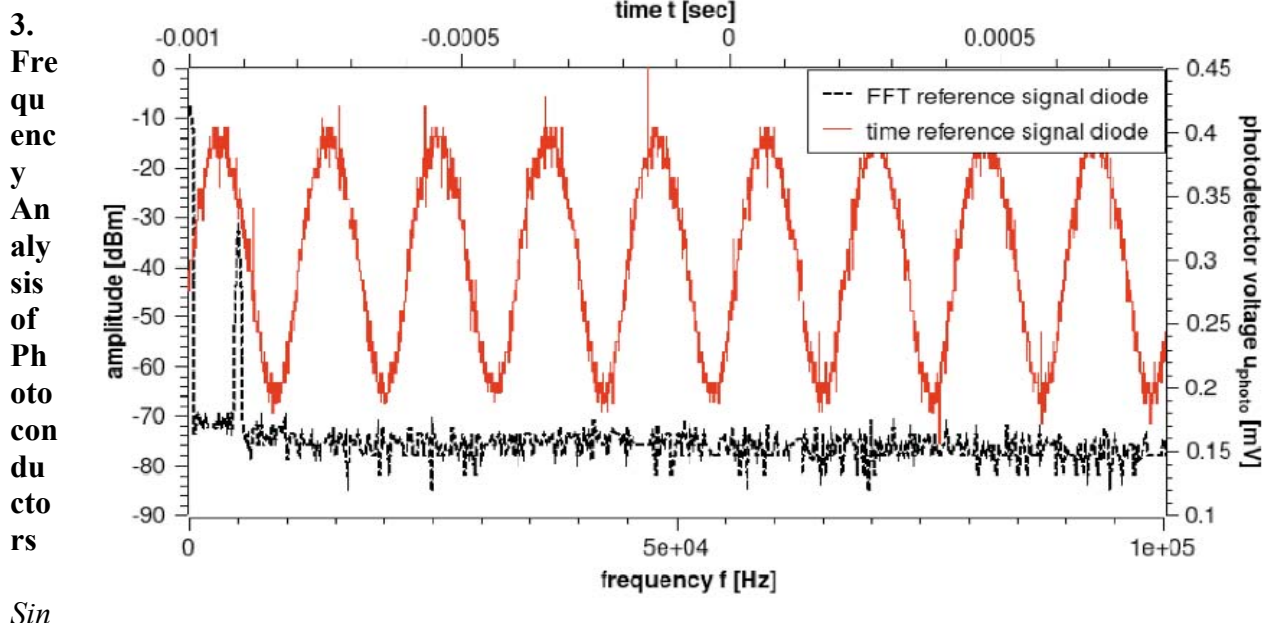


Figure 3 - 5kHz Sinusoidal Reference Signal from commercial photodetector

3. Frequency Analysis

As described in previous reports, initial tests of the fabricated photoconductors involved the detection of a 2.5 kHz square wave signal created by a cw laser passed through a chopper wheel. The frequency analysis of this modulated signal thus contained not only the 2.5kHz modulation frequency but also a large number of higher harmonics that formed the square wave signal. To simplify the analysis, the light source was modified as described in section 2.1 such that a sinusoidal single frequency waveform was incident on the photoconductor.

An electric amplifier circuit was designed to intensify both signal and noise coming from the photoconductor above the noise level of the used oscilloscope. The amplifier also reduces fluctuations of the bias-voltage of the measurement circuit by using batteries as source instead of wall-plug power-sources and shields the signal against surrounding radiation.

First, a 5kHz sinusoidal diode signal was measured with a commercial photodetector to provide a reference signal. The time and frequency components of the photodetector signal were analyzed, stored, and visualized with a CSA-7404 Tektronix 4 GHz-Oscilloscope. The data is shown in Figure 3.

The time reference signal (red line) is shown on the top using the right axis and the FFT signal (black dashes) is scaled on the bottom using the left axis.

The fabricated photoconductor was then tested using the same light source. The laser light was focused onto the device using a 0.25NA microscope objective to ensure that all of the light was incident on the detector. The signal from the GaAs-structure was measured by the bias circuit shown in **Error! Reference source not found.**

Next, the same procedure was applied to the fabricated photoconductor. Due to the size of the device, it was found that the incident light irradiated both the semiconductor region and the metal contacts. This caused a significant reduction in detected signal due to the creation of circular surface currents between the contacts. It is thought that this phenomenon is caused by the significantly larger resistance through the volume of the device than on the surface between adjacent “fingers” on the contact. To reduce this effect, rectangular slit apertures were placed in the beam path after the focusing objective to direct light onto certain regions of the device as shown in Figure 5. Apertures 1 and 2 were placed such that light was incident on only the “fingered” region of the contact with aperture 1 being larger than aperture 2. For the aperture bridge, apertures 1 and 2 were crossed such that light was incident only on exposed semiconductor material between two “fingers” of the contact.

As with the commercial device, a real time FFT was applied to the signal using the CSA-7404 Tektronix 4 GHz-Oscilloscope for frequency analysis. The electric response signal due to the laser-diode irradiation is shown in Figure 6 for all of the apertures used. It is important to notice that the response of the GaAs-semiconductor includes harmonics of the probe light signal. The reason for these harmonics is still under investigation.

Mid-IR Irradiation

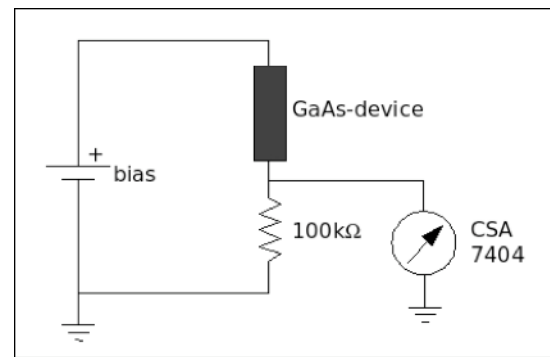


Figure 4 - Bias circuit

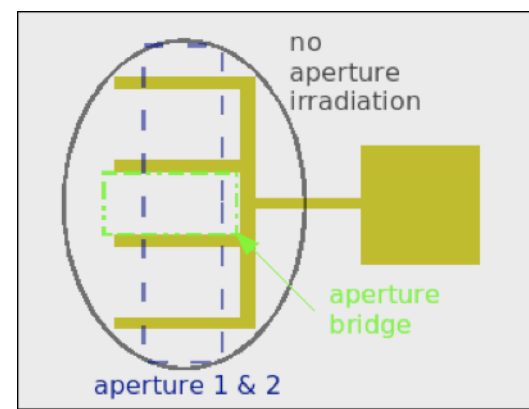


Figure 5 - Photoconductor device layout showing irradiated spots due to insert apertures

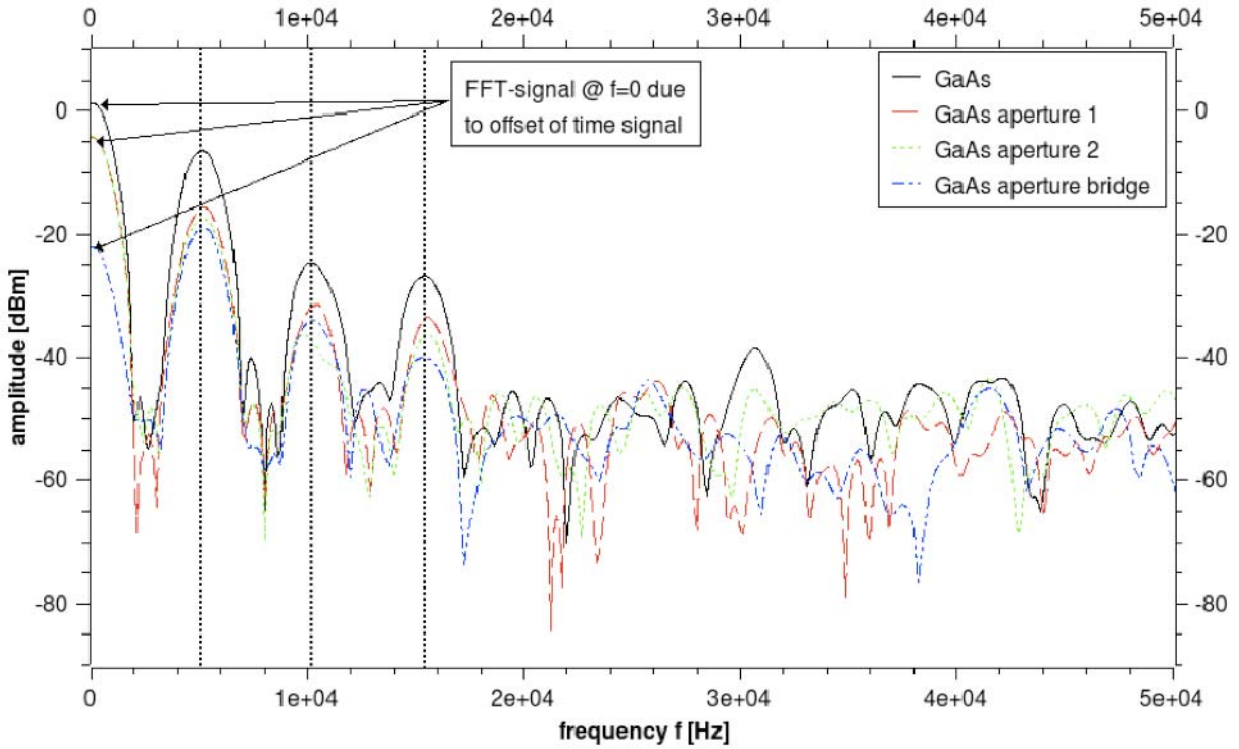


Figure 6 - Fourier-transformed electrical signal due to irradiation of the photoconductor with different apertures

In line with the original goal of the program for the laser passivation of photoconductors for the detection of mid-IR irradiation, the response of the fabricated photoconductors was tested with an incident light wavelength below the bandgap. To this end, a $2\mu\text{m}$ fiber laser described in section 2.3 was developed. The time domain signal and Fourier-transformed frequency response of this $2\mu\text{m}$ square wave signal modulated at a frequency of 1.5kHz are shown in Figure 7.

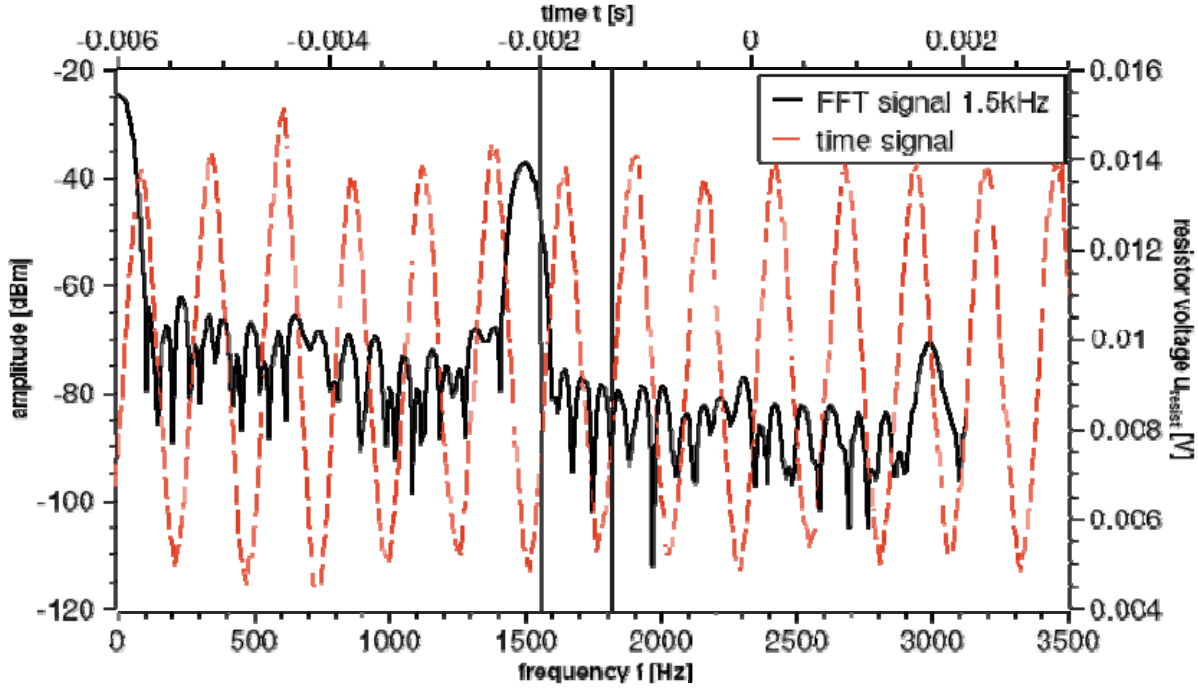


Figure 7 - Fourier-transformed electrical signal due to irradiation of the photoconductor with $2\mu\text{m}$ light

From the time response signal in [Error! Reference source not found.](#), it can be observed that the detected signal at $2\mu\text{m}$ more closely resembles the incident waveform than the detected signal at 632nm , as shown in Figure 8(a). However, the detector was not able to follow the square shape of the signal, which indicates a nonlinear response to the detected light.

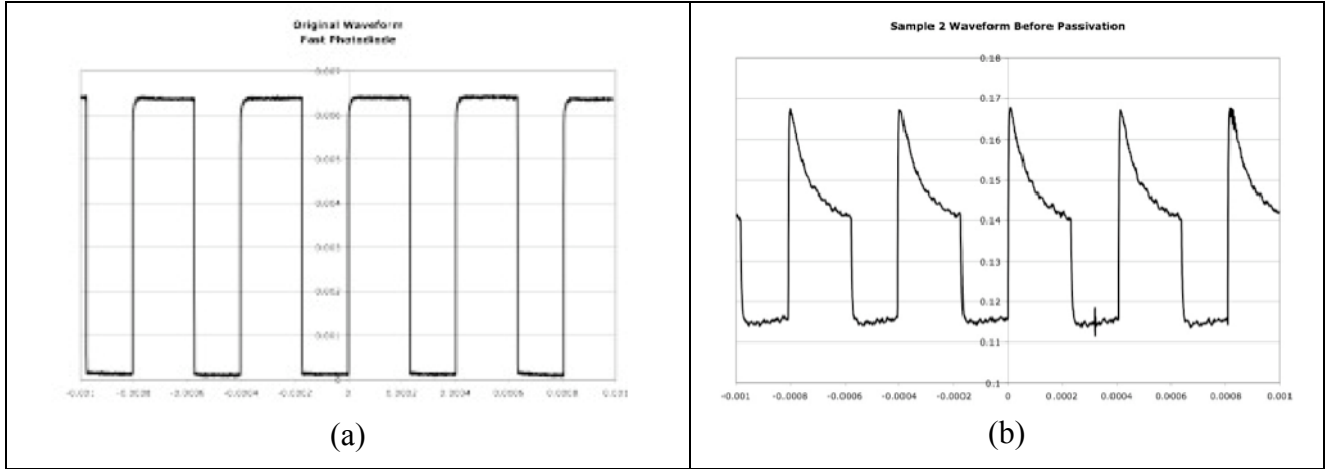


Figure 8 – (a) Reference signal of cw-beam from a 632nm HeNe laser source modulated with a chopper wheel acquired using a commercial photoconductor, (b) Signal of cw-beam from a 632nm HeNe laser source modulated with a chopper wheel acquired using a fabricated device

Dark Current Measurements

The observation of a nonlinear response in the previous experiments led to a reexamination of the electrical resistance properties of the fabricated photoconductors through an investigation of the I-V characteristic curves of the devices. Therefore, the previously performed dark current measurements of passivated and unpassivated devices were repeated using a low-noise battery as the bias source and the results are shown in Figure 9. These results indeed confirm the previous measurements with increased accuracy. The significantly different behavior of device #1 is due to surface ablation as a result of laser irradiation. For all devices, a highly nonlinear behavior is seen, which is believed to be due to the increased device thickness relative to commercial detectors.

Ultra-Low-Temperature Measurements

Noise measurements at ultra-low temperatures were taken to investigate the cutoff temperature for thermally generated free electrons in the

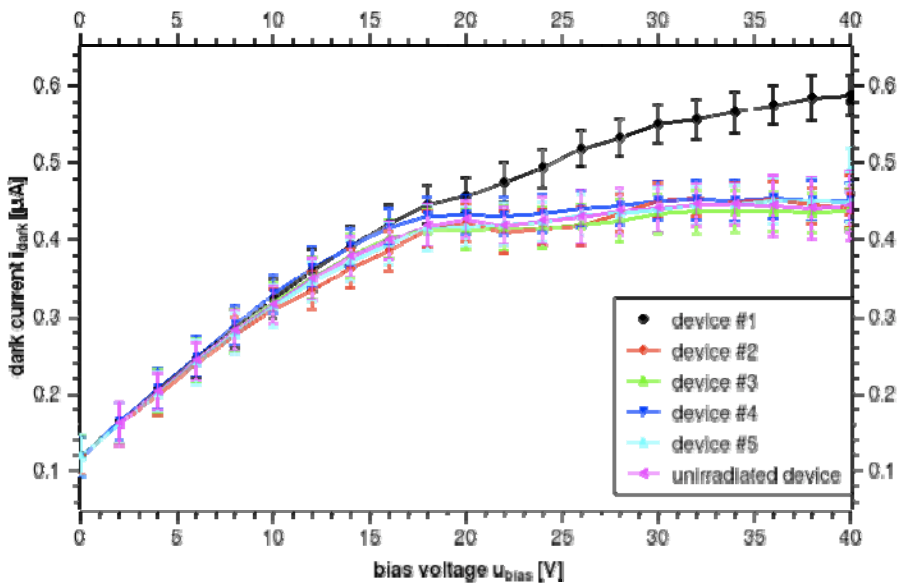


Figure 9 - Dark Current independent from heating the device

fabricated photoconductors before and after passivation. Below this cutoff temperature, thermal energy is not high enough to generate free electrons in a device. As passivation serves to “repair” dangling bonds that easily produce free electrons, a passivated device should have a higher cutoff temperature than an unpassivated device. Thus, this measurement serves as a qualitative means to describe the effectiveness of passivation. Below the cutoff temperature and in the absence of light, it is expected that no current will flow as thermal energy is insufficient to produce free electrons. Above the cutoff temperature, dark current will begin to flow with increasing voltage across the device and a nonzero I-V curve should be measurable. The dark current setup was the same as for previous experiments and is shown in Fig. 4. Beginning at a temperature of 15K, the bias voltage was varied from 0 to 20V and the dark current was measured. The temperature was then raised by 10K and the process repeated until a non-zero I-V curve was measured. Two devices were characterized in this initial experiment: a femtosecond laser passivated device with a laser fluence of 166.5mJ/cm^2 and an un-passivated device. The data at the lowest temperatures for which a non-zero I-V curve was measured are shown in Figure 10.

It can be seen that the passivated device has a *lower* cutoff temperature for thermally generated free electrons. Although there are only two curves, this would indicate that the laser parameters used for passivation in this case actually increases the number of dangling bonds rather than repairs them. Future work in this area should seek to verify this method as a means of determining the quality of passivation and ultimately using this measurement as a

metric for the optimization of laser parameters for the passivation of photoconductors.

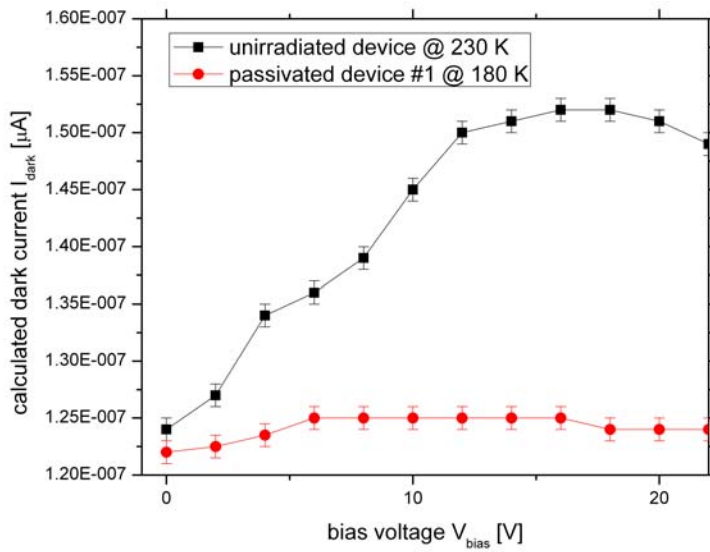


Figure 10 - Ultra-low Temperature Measurements

Conclusion and future work

The methods of analyzing the noise level and response of GaAs-semiconductor photoconductor were significantly improved and broadened.

- i) A nonlinear response due to light radiation on the photoconductors has been shown through an observed saturation behavior of dark current. It is believed that this nonlinear behavior is enhanced by the larger thickness of our fabricated photoconductors relative to commercial ones. Furthermore, the nonlinear device resistance is assumed to be responsible for the generation of higher harmonics in the detected signal. Further research is necessary to clarify this model.
- ii) The electronic response of our fabricated GaAs photoconductors to laser mid-IR illumination was demonstrated. It is assumed that the signal response does not arise from multi-photon absorption because of the low power of the incident light ($P_{\text{avg}} \approx 35\text{ mW}$). Rather, since the energy band-gap of GaAs is $E_{\text{gap}} = 1.4\text{ eV}$, the conduction electrons are most probably due to half-bound surface electrons of the outer shell of Arsenic. The analysis of the lattice structure near the surface of the GaAs-devices is ongoing.
- iii) Using a cryogenically cooled vacuum chamber, the temperature cutoff for the thermal

generation of free electrons in passivated and unpassivated devices was measured. It was found that passivation using current laser conditions *decreased* this cutoff temperature indicating a need to improve passivation parameters. The noise analysis still has to be improved to make a more precise analysis.

Next steps:

In addition to the ongoing experiments, the results suggest a need to investigate the following aspects:

- Because it was observed that the laser fluence used for passivation did not lead to sufficient passivation, increased laser dose on the material can be achieved by changing the **number of pulses** per spot on the sample during the irradiation process. This can be varied by adjusting the speed of the translation stage when passivating the surface. A decreased speed will result in a higher number of pulses per spot on the device.
- Irradiate the devices in an evacuated or low reactive environment to avoid recombination of surface electrons with particles in surrounding region. This can be accomplished by radiating the devices in a **vacuum chamber** or in an Argon flooded, sealed chamber. Micro X-ray diffraction (μ XD) spectroscopy should be used for a further investigation of the composition of the material after the fs-laser treatment.
- Inspection of the surface bond structure of the irradiated and unirradiated devices using **micro Raman** spectroscopy. This increases the understanding of the influences of fs-light pulses on the GaAs-lattice and the possible generation of half-bound electrons.
- A **change in the thickness** of the photoconductor devices. The used GaAs wafer has a thickness of $t=425\text{-}475\text{ }\mu\text{m}$. A reduction to $100\text{ }\mu\text{m}$ would decrease the probability of recombination of electron-hole pairs, which would also decrease the resistance of the devices, which yields an increase of the electric signal due to probe light. A use of thinner GaAs (111) wafer should be used to produce these new devices. Furthermore, a different orientation of the surface lattice supports the effects of fs-laser radiation because the cut of the lattice is not with a natural boundary of the crystal.